Cage Compounds

Deutsche Ausgabe: DOI: 10.1002/ange.201509057
Internationale Ausgabe: DOI: 10.1002/anie.201509057

The Regioselectivity of Bingel–Hirsch Cycloadditions on Isolated Pentagon Rule Endohedral Metallofullerenes

Marc Garcia-Borràs, Maira R. Cerón, Sílvia Osuna, Marta Izquierdo, Josep M. Luis,* Luis Echegoyen,* and Miquel Solà**

Abstract: *In this work, the Bingel–Hirsch addition of diethylbromomalonate to all non-equivalent bonds of $Sc_3N@D_{3h}$-C_{78} was studied using density functional theory calculations. The regioselectivities observed computationally allowed the proposal of a set of rules, the predictive aromaticity criteria (PAC), to identify the most reactive bonds of a given endohedral metallofullerene based on a simple evaluation of the cage structure. The predictions based on the PAC are fully confirmed by both the computational and experimental exploration of the Bingel–Hirsch reaction of $Sc_3N@D_{5h}$-C_{80}, thus indicating that these rules are rather general and applicable to other isolated pentagon rule endohedral metallofullerenes.*

Many endohedral metallofullerenes (EMFs) have been reported in the literature and they range from encapsulated single atoms to clusters of up to seven or eight atoms.[1] Computations have been crucial for the correct assignment and characterization of these compounds as they are usually obtained in low yields.[2] In EMFs, a formal charge transfer of up to six electrons from the metal cluster to the fullerene cage takes place, and is mainly responsible for their special properties and reactivity.[3]

In the last years, many EMFs with adjacent five-membered rings (5-MRs) have been synthesized. These EMFs do not obey the so-called isolated pentagon rule (IPR).[4] It has been recently demonstrated that the main reason behind the noncompliance of the IPR for EMFs is the aromaticity of the system: the more aromatic the negatively charged fullerene cages are, the more stable.[5] In addition, it has been proven that aromaticity can play a key role in the EMFs chemical reactivity.[5b]

The exohedral functionalization of EMFs has been extensively studied both experimentally and computationally.[2,6] The preferred addition sites are usually characterized by: a) short C−C bond lengths, b) relatively high pyramidalization angles, and c) appropriately shaped LUMOs.[6c,e] Depending on the fullerene cage and metal cluster encapsulated, the addition is preferred at sites that are far from (e.g. $Sc_3N@I_h$-C_{80}) or close to (e.g. $Y_3N@I_h$-C_{80}) the metal cluster.[6a,b]

Since the initial Bingel–Hirsch (BH) addition to $Gd@C_{60}$,[7] many EMFs have been functionalized using the same protocol.[8] However, there are some recent experimental and computational examples of BH additions to EMFs wherein the usually employed reactivity parameters are not able to explain the experimental observations. For instance, the BH addition to the non-IPR $Sc_3N@D_3(6140)$-C_{68}[8b,9] was found to occur at a [6,6] bond close to the Sc center.

In a recent report, Garcia-Borràs et al.[10] demonstrated that the thermodynamics of the BH addition to $Gd_3N@C_s(51365)$-C_{84}, having one adjacent pentagon pair (APP),[11] $Y_3N@C_2(22010)$-C_{78} with two APPs,[12] and $Sc_3N@D_3(6140)$-C_{68} with three APPs[13] is governed by the additive local aromaticity of the rings of the final adducts.[10] However, Alegret et al. found that BH additions are usually kinetically controlled, thus leading to the kinetic products instead of the most stable ones.[9]

Herein, we study the BH addition to all non-equivalent bonds of $Sc_3N@D_{3h}$-C_{78} using DFT calculations (see the Supporting Information for computational details). Based on these results and the subsequent analysis we introduce a practical and simple guide to predict the most suitable BH addition sites. As shown later, this guide only requires a simple evaluation of the EMF cage structure. We also performed the BH cycloaddition for the first time on the unexplored D_{5h} isomer of $Sc_3N@C_{80}$, and the synthesis and characterization of the resulting derivatives are described herein.

The Bingel–Hirsch addition of diethylbromomalonate to $Sc_3N@D_{3h}$-C_{78} was previously reported by Cai and co-workers.[8a] The C_{78}-based system presents the perfect platform to investigate this type of addition because the encapsulated metal cluster cannot freely rotate.[3] The BH reaction requires the presence of a base to deprotonate the malonate, and proceeds by a two-step mechanism (Figure 1 A). First, the bromomalonate reacts with the fullerene cage by nucleophilic addition to form a negatively charged intermediate (**INT**). This addition is a barrierless process.[9] Afterwards, the carbanion displaces the bromide and an intramolecular cyclopropane ring closure takes place.

In Figure 1 B, the reaction profile for the most favorable additions are represented (see Table S4 in the Supporting Information for the rest of the non-equivalent bonds of

[*] Dr. M. Garcia-Borràs, Dr. S. Osuna, Dr. J. M. Luis, Prof. Dr. M. Solà
Institut de Química Computacional i Catàlisi (IQCC) and Departament de Química, Universitat de Girona
Campus Montilivi, 17071 Girona, Catalonia (Spain)
E-mail: silvia.osuna@udg.edu
josepm.luis@udg.edu
miquel.sola@udg.edu
Dr. M. R. Cerón, Dr. M. Izquierdo, Prof. Dr. L. Echegoyen
Department of Chemistry, University of Texas at El Paso
El Paso, Texas 79968 (USA)
E-mail: echegoyen@utep.edu

Supporting information and ORCID(s) from the author(s) for this article are available on the WWW under http://dx.doi.org/10.1002/anie.201509057.

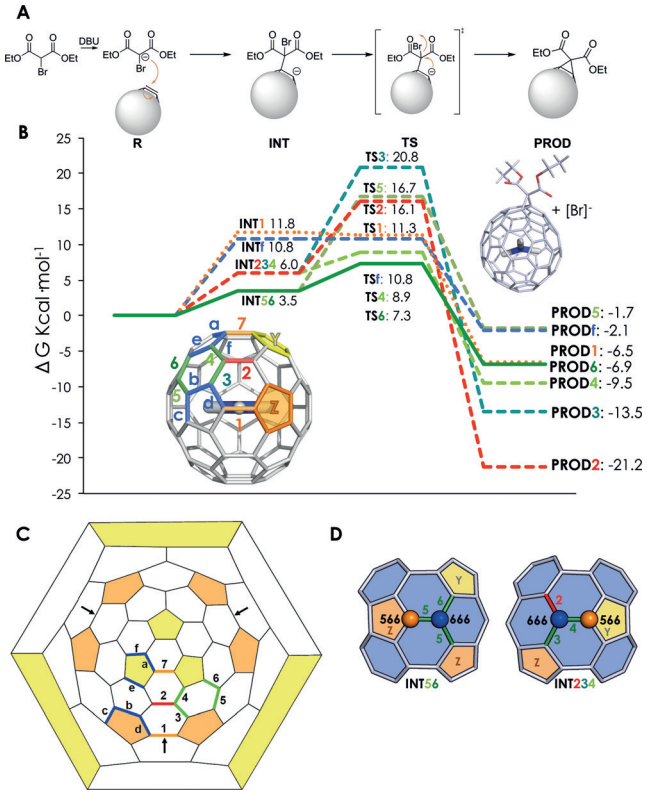

Figure 1. A) The Bingel–Hirsch mechanism. B) ΔG profile calculated at the BP86-D/TZP//BP86-D/DZP level of theory for the BH cycloaddition to selected non-equivalent bonds of $Sc_3N@D_{3h}$-C_{78} (in kcal mol^{-1}). C) Representation of the thirteen non-equivalent bonds of $Sc_3N@D_{3h}$-C_{78}. D) Schematic representation of intermediates **INT56** and **INT234**. Blue carbon atoms (in spheres) represent the initial addition site corresponding to C-666; orange carbon atoms denote C-566.

$Sc_3N@D_{3h}$-C_{78}). Experimentally, Cai and co-workers observed one monoadduct and one bisadduct, both corresponding to attack at the [6,6] bond labeled **6** (Figure 1C).[8a] Our calculations indeed indicate that the addition to bond **6** exhibits the lowest Gibbs activation barrier among all possible additions (7.3 kcal mol^{-1} with respect to isolated reactants). The addition to the [6,6] bond **4** exhibits a Gibbs activation barrier which is 1.6 kcal mol^{-1} higher. The rest of the non-equivalent positions exhibit even higher activation barriers. Interestingly, those bonds with lower activation barriers do not coincide with those having the most exothermic reaction energies. For instance, adduct **6** is the kinetically preferred isomer, whereas adduct **2** is thermodynamically the most stable.

The preferred BH cycloadduct corresponding to the addition to bond **6** exhibits an open-cage structure.[8a] As we recently demonstrated, the most stable adducts exhibit the largest aromaticities (see the Supporting Information).[10] Open-cage products are usually more aromatic than closed-cage ones, as the sp^2 hybridization of all fullerene carbon atoms is conserved.

As mentioned earlier, the BH reaction proceeds by a two-step mechanism. Each BH adduct can result from two different intermediates, depending on the carbon atom attacked by the bromomalonate (Figure 1D). Depending on the orientation of the malonate unit with respect to the neighboring fullerene carbon atom, three (or two in some cases due to symmetry) different final products can be obtained. The barriers for the interconversion of the different orientational isomers of malonate are very low and accessible at room temperature.[9] In addition, the differences in relative stabilities between different conformers are quite low (see Table S5 in the Supporting Information). The computed intermediates are about 3.5–11.8 kcal mol^{-1} higher in Gibbs energy than isolated reactants as a result of entropic effects (see Tables S3 and S4 in the Supporting Information).

Remarkably, the intermediate **INT56** (Figure 1D), which is the lowest in energy, leads to the kinetic BH adduct **6. INT56** and **INT234** are substantially more stable than the other possible intermediates. Both intermediates share the same feature: the addition occurs at a carbon atom situated among three hexagonal rings (we denote them as C-666). Our calculations show that aromaticity accounts for the extra stability of C-666 with respect to C-566 (i.e., the attacked carbon atom is among two hexagonal rings and one pentagonal ring). As expected, the negative charge transferred from the metallic cluster to the fullerene cage is mainly localized on the 12 5-MRs (see Table S1 in the Supporting Information). Aromaticity estimations using the NICS and MCI indexes presented in Table S2 indicate that 5-MRs are more aromatic than 6-MRs.[6d] Thus, if a C-566 intermediate is formed, the process will be disfavored because of greater disruption of the aromaticity.

A second key factor in explaining the stability of the intermediates should be taken into account, that is, the BH initial intermediate has one negative charge, which is delocalized in the vicinity of the carbon atom undergoing the attack. Therefore, those intermediates exhibiting 5-MRs on neighboring positions will be able to better stabilize this extra negative charge. The location of the 5-MRs is the main reason for the extra stability of **INT56**, which is almost 3 kcal mol^{-1} more stable than **INT234**. The latter has two pentagonal rings and one hexagonal ring in neighboring positions, while **INT56** exhibits three pentagonal rings (Figures 1D; see Figure S1).

The lowest-energy **INT56** could lead to the formation of either **5** or **6**, but the activation barrier that leads to **5** is almost 10 kcal mol^{-1} higher than the one corresponding to **6**. As discussed, the negative charge is mainly localized across 5-MRs. The charge distribution on 5-MRs is, however, not uniform: those rings situated close to the metal atoms (denoted as Z rings in Figure 1B) are the ones exhibiting a higher negative charge [q_{Bader}(Z-5-MR) = −0.415 e and q_{Bader}(Y-5-MR) = −0.115 e; Table S1]. This higher charge is localized on the Z rings, thus making Z-5-MRs more aromatic, and therefore the ring closure during the second step of the BH is preferred for the less aromatic Y-5-MRs (Table S2). The final BH product results from the intermediate which disrupts the aromaticity the least during the first step of the reaction (**INT56**), and the transition state for ring-closure at the less aromatic 5-MR (**TS6**) dictates the preferred addition site. For intermediate **INT234**, the ring closure on 5-MRs is preferred over that of 6-MRs even though the latter

rings are less aromatic because 6-MRs have a much lower nucleophilic character than 5-MRs (TS2 > TS4 > TS6).

The understanding of the $Sc_3N@D_{3h}$-C_{78} BH reactivity patterns allow us to propose a set of aromaticity-based criteria, the predictive aromaticity criteria (PAC), for the BH addition on IPR EMFs (Figure 2). The PAC identify the lowest-energy intermediates and transition states for a given EMF by a simple visual inspection of the initial fullerene structure.

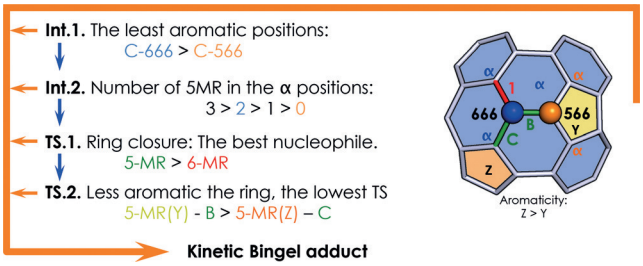

Figure 2. Predictive aromaticity criteria (PAC) for the Bingel–Hirsch addition to IPR EMFs.

The most aromatic (and therefore lowest in energy) intermediates lead to the lowest activation barriers for the BH addition. The PAC criteria states that: 1) the lowest-energy intermediate should be located in a 666 region (C-666), and 2) among all possible C-666s, those possessing more pentagonal rings adjacent to the 666 region (denoted as α-positions in Figure 2) will likely be more favored. The penalty for having fewer adjacent 5-MRs is, however, small, as it ranges between 2–3 kcal mol^{-1}. According to PAC, the lowest-energy transition states for the cyclopropane ring closure will occur on: 1) 5-MRs and 2) among all 5-MRs, those located far from the metal cluster. These rings will therefore exhibit a lower aromaticity and less-negative charge (i.e. Y-5-MRs are preferred over Z-5-MRs). Application of the PAC to the BH addition to $Sc_3N@I_h$-C_{80} predicts that the [6,6] bond is the most reactive in complete agreement with experimental and theoretical studies.[9]

We also used the PAC to predict the preferred BH additions to the challenging $Sc_3N@D_{5h}$-C_{80}. This C_{80} isomer exhibits nine non-equivalent bonds (five are [6,6] bonds and four [5,6]), and the cluster unit can freely rotate inside.[3] Among all nine possible additions, five (out of nine) bonds can be immediately discarded by just applying the PAC. The BH adducts exhibiting the lowest activation barriers will be those coming from one of the two possible C-666 positions (**INT12** and **INT34**; Figure 3). Therefore, PAC predicts products **1**, **2**, **3**, and **4** as possible BH candidates. **INT34** might be slightly more stable than **INT12** since it has one additional 5-MR adjacent to the 666 region. According to the PAC, the formation of **1** would be disfavored as the final cyclopropane ring formation involves attack of a 6-MR. In addition, as the 5-MR rings, which contain bond **b**, are more aromatic than the 5-MR rings containing bonds **a**-**c**-**d** (see Table S6 in the Supporting Information), the PAC predicts that the cyclopropane closure from **INT34** to form **3** should be more favorable.

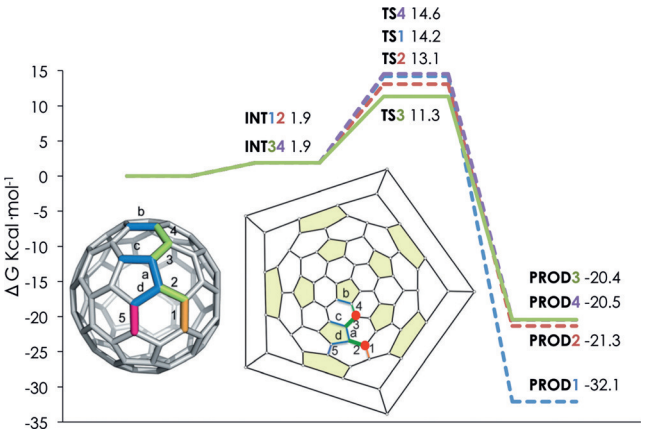

Figure 3. Gibbs energy profile calculated at the BP86-D/TZP//BP86-D/DZP level of theory for the BH cycloaddition to selected non-equivalent bonds of $Sc_3N@D_{5h}$-C_{80} (in kcal mol^{-1}) and the representation of the five non-equivalent [6,6] bonds: pyrene bond type bond **1**; pyracylene bond **5**; type B bonds **2**, **3**, **4**, and **5**; and four [5,6] type D corannulene bonds **a**–**d**.

We computed the reaction paths for all nine possible additions, considering seven different orientations of the inner metal cluster (see Table S7 in the Supporting Information). The intermediates **INT12** and **INT34** are indeed the most stable, as predicted from the PAC, and they are more than 3 kcal mol^{-1} lower in energy than the other possible intermediates (Table S7). Moreover, the TSs corresponding to the additions towards bonds **1**, **2**, **3**, and **4** are the lowest in energy, in accordance to what was predicted by the PAC (Table S7). For the most favorable additions we have computed the complete Gibbs reaction profiles, as reported in Figure 3. For these four additions, the corresponding intermediate is 1.9 kcal mol^{-1} less stable than isolated reactants, and **TS3** is the one presenting the lowest activation barrier. Thus, as predicted by the PAC and confirmed by DFT calculations, the addition to bond **3** is the preferred BH kinetic product. Product **3** is, however, not the most stable thermodynamic product ($\Delta G_R = -20.4$ kcal mol^{-1}, while $\Delta G_R = -32.1$ kcal mol^{-1} for product **1**).

The final proof of the validity of the PAC for predicting BH additions to EMFs was provided by the experimental BH functionalization of $Sc_3N@D_{5h}$-C_{80}. Bromoethylmalonate and DBU were added to an *o*-dichlorobenzene solution of pure $Sc_3N@D_{5h}$-C_{80}.[14] Three different monoadduct isomers [**A** (21%), **B** (15%), and **C** (6%)] were purified and characterized by ^{1}H NMR spectroscopy and UV/vis. The ^{1}H NMR spectrum of the major product, **A**, proved that the compound possesses an unsymmetric addition pattern. Consequently, addition to the symmetric [6,6] bonds **1**, **4**, and **5** can be ruled out, and only the unsymmetric [6,6] **2**, **3** bonds and [5,6] **a**–**d** bonds remain as possibilities. According to the computational results, all [5,6] additions are discarded. Moreover, calculations show that addition to bond **2** has a Gibbs barrier which is 1.8 kcal mol^{-1} higher than that for the addition to bond **3**. Thus, the results from NMR spectroscopy, combined with the computed activation barriers and the PAC predictions point to the same conclusion: the major BH product **A** corresponds to the addition to the unsymmetric bond **3**.

The ^{1}H NMR spectrum of **B** proved that the compound results from a symmetric addition pattern. Therefore, addition to symmetric [6,6] bonds **1**, **4**, and **5** would be consistent with the observed NMR spectrum. Based on DFT calculations, addition to the [6,6] bond **5** can be discarded. The attack on bond **4** is in direct competition with that at bond **3**, as they share the same intermediate **INT34**. Thus, once the intermediate is formed, the preferred attack corresponds to that at bond **3** ($\Delta G^{\ddagger} = 11.3$ kcal mol^{-1}), for which the TS is 3.3 kcal mol^{-1} lower in energy than the one for the addition to bond **4** (Figure 3). Consequently, all evidence supports that the experimentally isolated isomer **B** corresponds to the monoadduct **1** ($\Delta G^{\ddagger} = 14.2$ kcal mol^{-1}), which has a TS that is 0.4 kcal mol^{-1} lower in energy than the one corresponding to that obtained for attack at bond **4**.

The ^{1}H NMR spectrum of **C** exhibited two quartets corresponding to the methylene of the ethyl ester groups. As explained before, by combining the symmetry considerations from the ^{1}H NMR spectrum and DFT calculations, we suggest that **C** corresponds to addition to the unsymmetric bond **2**.

The isomers **A**, **B**, and **C** showed essentially identical UV/Vis absorption spectra to that observed for the pristine fullerene $Sc_3N@D_{5h}$-C_{80}, thus indicating that the additions for **A**, **B**, and **C** are likely to yield adducts with open bonds in agreement with DFT predictions (see Table S7).[15]

Based on the analysis of the BH derivatization of $Sc_3N@D_{3h}$-C_{78} EMF in terms of aromaticity and nucleophilicity, a set of simple rules to predict the most favorable BH addition sites from a simple evaluation of the cage structure has been proposed. The PAC was used to predict the BH regioselectivity in the $Sc_3N@D_{5h}$-C_{80} system. The PAC predicted bond **3** to be the one most favored, and was later confirmed by an extensive computational study of the BH reaction and by experimental functionalization. The excellent agreement between the PAC predictions, the experimental assays, and DFT calculations indicate that these rules are rather general and applicable to other BH additions on IPR EMFs.

Acknowledgements

We are grateful to the Spanish MINECO (CTQ2014-54306-P, CTQ2014-52525-P, CTQ2014-59212-P, and JdlC contract to S.O.), the Catalan DIUE (2014SGR931, ICREA Academia 2014 Award to M.S. and XRQTC), and the FEDER fund (UNGI10-4E-801) for financial support. M.G.-B. thanks the Spanish MECD for a PhD grant (AP2010-2517) and S.O. the European Commission for CIG project (FP7-PEOPLE-2013-CIG-630978). CESCA and BSC-CNS are acknowledged. M.R.C, M.I. and L.E. thanks the NSF for generous support of this work under grant (CHE-1408865) and to the NSF-PREM program (DMR-1205302). The Robert A. Welch Foundation is also gratefully acknowledged for an endowed chair to L.E. (grant AH-0033).

Keywords: aromaticity · cage compounds · density-functional calculations · fullerenes · supramolecular chemistry

How to cite: *Angew. Chem. Int. Ed.* **2016**, *55*, 2374–2377
Angew. Chem. **2016**, *128*, 2420–2423

[1] X. Lu, L. Feng, T. Akasaka, S. Nagase, *Chem. Soc. Rev.* **2012**, *41*, 7723–7760.
[2] a) A. Rodríguez-Fortea, A. L. Balch, J. M. Poblet, *Chem. Soc. Rev.* **2011**, *40*, 3551–3563; b) S. Osuna, M. Swart, M. Solà, *Phys. Chem. Chem. Phys.* **2011**, *13*, 3585–3603.
[3] J. M. Campanera, C. Bo, M. M. Olmstead, A. L. Balch, J. M. Poblet, *J. Phys. Chem. A* **2002**, *106*, 12356–12364.
[4] H. W. Kroto, *Nature* **1987**, *329*, 529–531.
[5] a) M. Garcia-Borràs, S. Osuna, M. Swart, J. M. Luis, M. Solà, *Angew. Chem. Int. Ed.* **2013**, *52*, 9275–9278; *Angew. Chem.* **2013**, *125*, 9445–9448; b) M. Garcia-Borràs, S. Osuna, J. M. Luis, M. Swart, M. Solà, *Chem. Soc. Rev.* **2014**, *43*, 5089–5105.
[6] a) S. Osuna, R. Valencia, A. Rodríguez-Fortea, M. Swart, M. Solà, J. M. Poblet, *Chem. Eur. J.* **2012**, *18*, 8944–8956; b) S. Osuna, M. Swart, M. Solà, *J. Am. Chem. Soc.* **2009**, *131*, 129–139; c) S. Osuna, M. Swart, J. M. Campanera, J. M. Poblet, M. Solà, *J. Am. Chem. Soc.* **2008**, *130*, 6206–6214; d) M. Garcia-Borràs, S. Osuna, M. Swart, J. M. Luis, M. Solà, *Chem. Commun.* **2013**, *49*, 1220–1222; e) M. Garcia-Borràs, S. Osuna, J. M. Luis, M. Swart, M. Solà, *Chem. Eur. J.* **2012**, *18*, 7141–7154.
[7] R. D. Bolskar, A. F. Benedetto, L. O. Husebo, R. E. Price, E. F. Jackson, S. Wallace, L. J. Wilson, J. M. Alford, *J. Am. Chem. Soc.* **2003**, *125*, 5471–5478.
[8] a) T. Cai, L. Xu, C. Shu, H. A. Champion, J. E. Reid, C. Anklin, M. R. Anderson, H. W. Gibson, H. C. Dorn, *J. Am. Chem. Soc.* **2008**, *130*, 2136–2137; b) T. Cai, L. Xu, C. Shu, J. E. Reid, H. W. Gibson, H. C. Dorn, *J. Phys. Chem. C* **2008**, *112*, 19203–19208; c) O. Lukoyanova, C. M. Cardona, J. Rivera, L. Z. Lugo-Morales, C. J. Chancellor, M. M. Olmstead, A. Rodríguez-Fortea, J. M. Poblet, A. L. Balch, L. Echegoyen, *J. Am. Chem. Soc.* **2007**, *129*, 10423–10430; d) N. Alegret, M. N. Chaur, E. Santos, A. Rodríguez-Fortea, L. Echegoyen, J. M. Poblet, *J. Org. Chem.* **2010**, *75*, 8299–8302.
[9] N. Alegret, A. Rodríguez-Fortea, J. M. Poblet, *Chem. Eur. J.* **2013**, *19*, 5061–5069.
[10] M. Garcia-Borràs, S. Osuna, M. Swart, J. M. Luis, L. Echegoyen, M. Solà, *Chem. Commun.* **2013**, *49*, 8767–8769.
[11] T. Zuo, K. Walker, M. M. Olmstead, F. Melin, B. C. Holloway, L. Echegoyen, H. C. Dorn, M. N. Chaur, C. J. Chancellor, C. M. Beavers, *Chem. Commun.* **2008**, 1067–1069.
[12] A. A. Popov, M. Krause, S. Yang, J. Wong, L. Dunsch, *J. Phys. Chem. B* **2007**, *111*, 3363–3369.
[13] M. M. Olmstead, H. M. Lee, J. C. Duchamp, S. Stevenson, D. Marciu, H. C. Dorn, A. L. Balch, *Angew. Chem. Int. Ed.* **2003**, *42*, 900–903; *Angew. Chem.* **2003**, *115*, 928–931.
[14] a) M. R. Cerón, F.-F. Li, L. Echegoyen, *Chem. Eur. J.* **2013**, *19*, 7410–7415; b) M. R. Cerón, M. Izquierdo, N. Alegret, J. A. Valdez, A. Rodríguez-Fortea, M. M. Olmstead, A. L. Balch, J. M. Poblet, L. Echegoyen, *Chem. Commun.* **2016**, *52*, 64–67.
[15] a) M. Izquierdo, M. R. Cerón, M. M. Olmstead, A. L. Balch, L. Echegoyen, *Angew. Chem. Int. Ed.* **2013**, *52*, 11826–11830; *Angew. Chem.* **2013**, *125*, 12042–12046; b) M. Chen, X. Lu, M. R. Cerón, M. Izquierdo, L. Echegoyen, *Endohedral Metallofullerenes*, CRC Press, Boca Raton, FL, **2014**, pp. 173–210.

Received: September 27, 2015
Published online: January 14, 2016

